JTTEES 5:196-206


# Peel Strength of Thermal Sprayed Coatings

*M. Sexsmith and T. Troczynski*

**For the thermal spray industry to progress, informative and reliable coating evaluation techniques are needed. Measurement of adhesion is an important function, and existing tests have severe limitations. The peel adhesion test (PAT) was adapted to thermal spray coatings (TSC) from the adhesives industry. In this test, a thin metal foil is coated by thermal spraying. The foil is then peeled off the coating at a constant speed. The force required for separation is monitored as a function of crack position. The force is than converted into a peel strength that is equivalent to the energy required for separation. The adhesion of a range of different TSCs was measured in the form of spray pattern profiles and uniform coatings. Results were compared with the ASTM standard for TSC adhesion measurement, the expected range of interface toughness, and the Vickers hardness of the coating. Comparisons indicate that the PAT is self consistent, and it produces results comparable to other toughness measurements. The peel test was used to determine interface toughness in the range of 10 to 60 J/m$^2$ for ceramic coatings, 150 to 250 J/m$^2$ for cermet coatings, and 160 to 300 J/m$^2$ for metal coatings.**

## 1. Introduction

ADHESION of thermal spray coatings is an important problem facing engineers who design coated components. Adhesion is affected by a host of variables including powder and torch parameters, surface preparation, and substrate heating. An understanding of how these variables interact is necessary for coating users to have confidence in the product. Traditional adhesion measurement techniques are useful to compare coating quality, but are limited in their use for predictions. A new peel adhesion test is proposed to address the need for a more informative test. A fundamental problem in investigating adhesion is to define or select a parameter that characterizes the strength of an interface. Normally the choice of parameter is limited by the accepted tests (Ref 1), and it is difficult to convince a conservative industry that a new parameter is a better measure of adhesion. Because of these constraints, an adhesion test should meet certain requirements. The test should be easy to perform and should not require expensive equipment or sophisticated analysis. Industry will not be willing to accept sophisticated tests that require substantial employee training or capital investment. The tested component should represent the actual components sprayed. Most destructive tests are performed on coupons that have a very different size and shape than the engineered components. The test should be sensitive only to adhesion and not to other closely related variables such as residual stress. This will allow the effects of these other variables to be understood independently. The measured parameter should be useful in predicting service limitations. Thus, the cause of failure in the test should be understood so that a theory describing the failure process can be used to predict the failure of an engineered component.

The variables that affect bonding must be identified to understand adhesion. With most adhesive systems, this list includes three categories. The first category is the chemical compatibility of the two materials. This is usually characterized by the types of chemical bonds that can form between them. In systems where one material was liquid at the time of bonding, the chemical interaction with the surface is characterized by the wetting angle. Low wetting angle interfaces would be more strongly adherent than high angle interfaces. The cleanliness of the surface is very important in determining wetting angle and, thus, the bonding. The second category is the mechanical nature of the interface. In thermal spraying, the surface is grit blasted before coating to provide a rough surface onto which the coating can mechanically lock. Grit blasting disturbs any layer on the surface and exposes the more active material underneath. The impact of the particles assists in this interlock process, and processes with high speed particles tend to produce better bonding. The surface ductility controls the nature of this roughening process. The third category is the loading on the interface. The applied external loads can be aggravated by the internal residual stresses generated during processing. The residual stresses are caused by rapid quenching of the particles and by the large thermal gradients produced during spraying. For thick coatings, the residual stresses can be high enough to fail the coating either by spalling or cracking.

**Keywords** adhesion, fracture mechanics, interface toughness, peel testing

**M. Sexsmith** and **T. Troczynski,** Department of Metals and Materials Engineering, University of British Columbia, 309-6350 Stores Rd., Vancouver, B.C. V6T 1Z4 Canada. M. Sexsmith is now with Ballard Adv. Materials, North Vancouver, B.C., Canada.

## 2. Peel Testing of Adhesion

An adhesion test should have the predictive ability of the fracture mechanics tests and the simplicity of the force based tests. The peel test has both qualities. Several standard test configurations exist (Ref 2, 3). Many studies on the mechanics of the test system were undertaken (Ref 4-7) because of its widespread use in the adhesives industry. In a peel test, a thin adherend is pulled from its substrate, in this case a coating, with a fixed geometry. The crack propagates in a stable manner at the peel speed. Figure 1(a) shows the basic principle. The force required to continue cracking is monitored as a function of crack position and time. The peel test produces a force versus displacement curve that represents the adhesion of the coating. The resulting peel strength represents the incremental energy per unit width per increment peeled and has the units of N/m. This is

equivalent to the surface energy with units of $J/m^2$. Because very little energy is stored in the bent foil, crack propagation is stable and controlled by the displacement of the sample.

The peel test essentially measures the average adhesion along the line of the crack tip. As the crack progresses, a different portion of the interface is loaded. The test can be used to map the adhesion in the direction perpendicular to the crack front by measuring the load as a function of crack position. This allows the detection of surface inhomogeneities that affect adhesion. Resolution of the test depends on the size of the area of foil that is loaded, which in turn depends on the geometry of the peel test. Peel testing traditionally has been used to measure the adhesion of tapes and glue (Ref 4-6), and most manufacturers of adhesives list the peel strength of their products alongside lap shear and tensile strength. Because of the simplicity of the test, attempts have been made to apply the peel test to other coating systems. In the microelectronics industry, a peel test is used to evaluate the bonding of metal films to ceramics (Ref 8). The test also was applied to thin film coating systems where the coating is peeled from the substrate (Ref 7). In these tests, the coating itself is peeled from the substrate. The peel stresses and forces depend largely on the coating properties, and stable peeling was not always possible.

Among the available peel tests, two basic forms exist. They are similar in terms of sample preparation and procedure but can generate very different crack tip stresses. In the first form, the compliant adherend is peeled from the substrate at a specified angle. In most cases, the angle is 90° (T-peel) or close to 0° from the substrate plane. The shape of the adherend is controlled by its properties and the properties of the interface and substrate. The stress intensity at the crack tip and the amount of plastic work performed to bend the adherend for a given peel load is a function of all the materials properties of the system and the peel angle. This geometry is very similar to a double cantilever beam test. One beam, though, is extremely compliant, and the other beam is infinitely stiff. In the second form (used in this work), the compliant adherend is bent around a rotating mandrel (Fig. 1b and c); therefore, the shape of the deformed adherend is controlled. The tensile force in the adherend is measured in this test. The strains in the adherend conforming to a mandrel are usually much smaller than in the free peeling tests. In this case, the amount of plastic work depends on the adherend properties only and can be controlled by changing the mandrel size. The stress intensity at the crack tip depends on the properties of all of the materials involved, but because of the smaller strains, the mechanical description of the system is simpler.

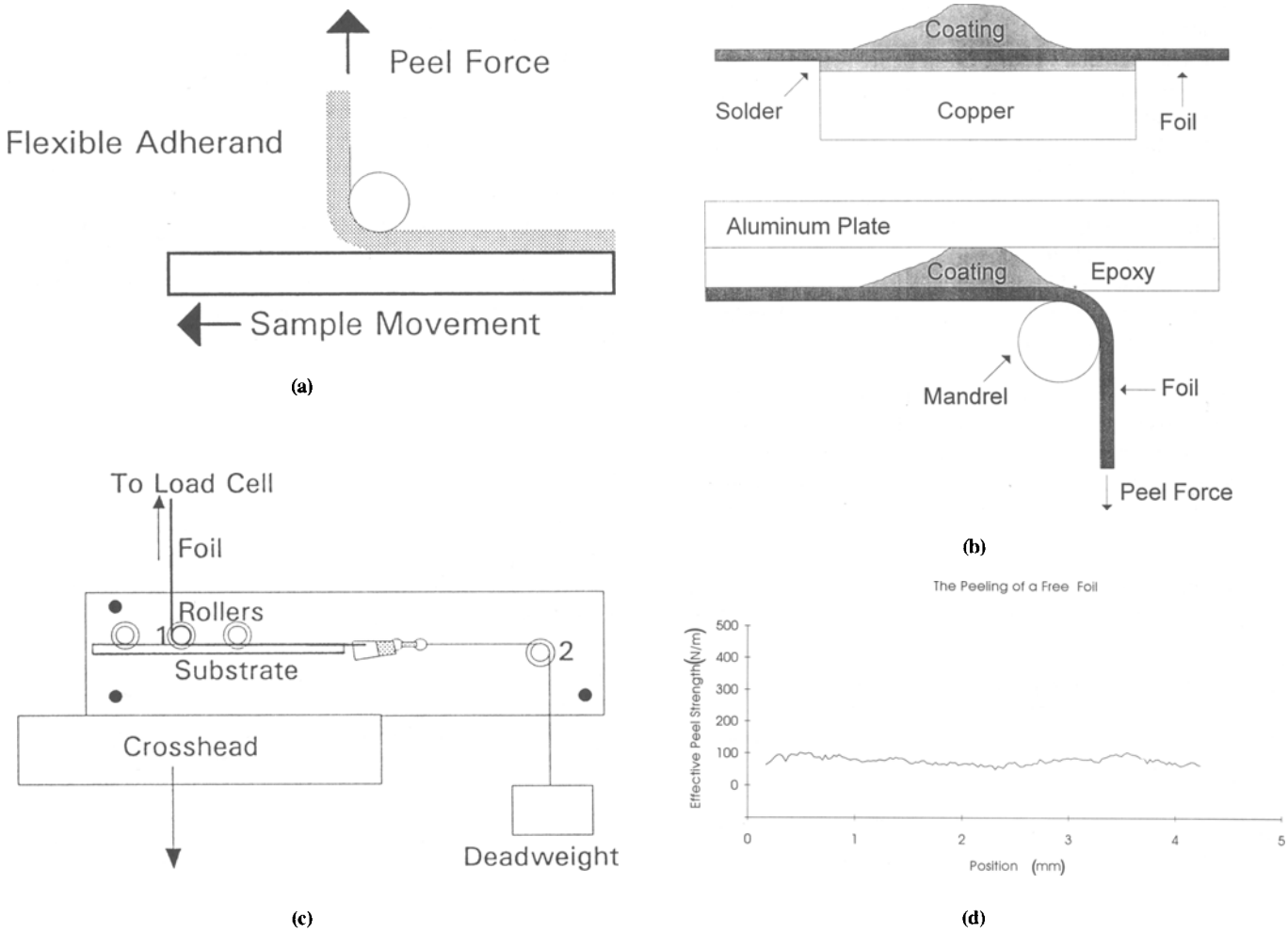


**Fig. 1** Principles of the PAT (a) peeling around a mandrel, (b) PAT sample preparation, (c) PAT loading jig, and (d) PAT calibration through peeling of a free foil

## 3. Peel Adhesion Test (PAT) for Thermal Sprayed Coatings (TSC)

Several experimental procedures of the PAT were developed in this work. They are all described in detail in previous publications (Ref 9-12); thus, only a brief description of PAT is given here. Several new procedures were developed to coat and test a thin foil to adapt the peel test to the TSC. The geometry of peeling has a significant effect on the failure of the interface. By changing the foil loading, the state of crack tip stress changes, and thus, the measured parameter may change its meaning. For a constant peeling geometry, however, the type of stress is not expected to vary much with the level of adhesion (Ref 5). It is easier to control the geometry with a mandrel-type test (Fig. 1b and c); thus, the geometry used was based on the ASTM D 3167 floating roller peel test.

The loaded region should be small to ensure controlled crack propagation along the interface. A small radius mandrel (6.35 mm diam) was used to maximize foil strain at the interface within a small, well-defined region. Thin foils reduce the amount of plastic work dissipated in the test and make it easier to ensure that the foil conforms to the mandrel. Thin foils, however, are fragile and difficult to handle. Several foil thicknesses were examined. The PAT, at the current state of development, works for foils between 50 and 250 μm, and a 75 μm foil was the easiest to use.

The selection of a suitable substrate is critical because of the limited number of available foil materials. The thin foil test substrate should behave mechanically and chemically like the bulk substrate. Because of the wide variety of substrate materials sprayed, it is impossible to find a single foil type that would represent the bonding to these materials Since most of these materials are not available in a thin foil form, a 302 stainless steel foil was chosen as a substrate in this work. Several other foils, including pure nickel (Ni), brass, and aluminum (Al),were examined to explore the effect of substrate material on bonding. The brass and Al foils were difficult to work with, and while it was possible to use them, they were not tested extensively. The pure Ni foil was an excellent substrate for this test.

Peel tests require that one adherend is sufficiently compliant and that little energy is lost to bending the adherend compared to the bonding energy. To provide mechanical backing and a thermal sink, the PAT foil was soldered to a copper block (Fig. 1b) and grit blasted with 100 grit $Al_2O_3$ at 560 kPa (80 psi) at a distance of 80 mm at 45° from the surface. This grit blasting angle was maintained constant for all the PAT samples presented in this work. A further PAT study is planned to determine the effects of grit blasting conditions on peel adhesion of the TSC. Care was taken to grit blast each sample in an identical fashion. The coatings were applied using several different torches to allow a range of coating processes to be explored. Previous reports (Ref 9, 11) included PAT results for coatings produced using traditional radial injection plasma torches. In this work, the coatings were produced using two axial injection plasma torches (Axial III by Northwest Mettech, Richmond, B.C. V6V 1M3, and AxiJet by Metcon Services, Abbotsford, B.C. V2S 1M3) and Rokide oxygen/acetylene torch by Norton, Worcester, MA 01615-0008. The powders and coating types sprayed at each facility were different; thus, comparisons between them are inappropriate.

Two types of samples were sprayed for each coating type. The first sample, the "profile sample," is prepared by holding the torch stationary and moving the substrate along one axis. A Gaussian-shaped band of coating is formed; it is represented schematically in Fig. 1(b). This geometry allows the variation in adhesion between different portions of the plasma stream to be measured. The second type of sample was an ordinary "uniform coating." Thickness of the uniform coatings, equivalent to the maximum thickness of the profile coating, is provided in Table 1. In addition to the peel test samples, several mild steel bars and ASTM C 633 (Ref 13) cylinders were coated. From these extra samples, other traditional evaluations could be made, such as hardness, microstructure, and a comparative bond strength test.

The sprayed samples were cleaned with alcohol and glued using a thermoset epoxy (type EC1386, by 3M Corp., Saint Paul, MN) to a clean, grit-blasted, 1 mm thick Al plate. Viscosity of the epoxy was large enough to prevent penetration into porous coatings, such as thermal barrier coatings. Lack of penetration of the epoxy into the coatings was confirmed by microscopic observations (optical micrograph and scanning electron microscope, SEM) of the polished sections. After the glue was cured, the samples were placed on an electric hot plate until the solder melted. The Al, glue, coating, and foil sandwich were separated from the copper block (Fig. 1b), and the melted solder was quickly brushed off the foil using steel wool. The edges of the sandwich were ground parallel on a wet silicon carbide wheel to reduce the possibility of edge effects. The size of the damage zone was minimized by grinding with successively smaller grits. The sample was mounted in the jig (Fig. 1c), and the starting tab was clamped into the jaw. The foil was pulled from the coating at a constant rate of 2.5 mm/min. The load and crosshead displacement were monitored and recorded digitally. For each type of foil, a calibration was performed, as in Fig. 1(d). It involved passing a sample with zero peel strength through the

**Table 1 Summary of representative test data**

| Coating type | Sprayer | Coating thickness, mm | HV300 | ASTM bond strength, MPa | Peel strength, N/m | |
|---|---|---|---|---|---|---|
| | | | | | Stainless steel foil | Ni foil |
| $Cr_2O_3$ | Metcon | 0.080 | 822 | >70 | 40 | 193 |
| $Cr_2O_3$ | Rokide | 0.128 | 1067 | >70 | 36 | 254 |
| $Cr_2O_3$ | Mettech | 0 230 | NA | 45 | NA | NA |
| NiCr-$Al_2O_3$ | Rokide | 0 300 | 247 | 46 | 280 | 486 |
| Fe bond coat | Mettech | 0 121 | 123 | >70 | 213 | 718 |
| Titanium | Metcon | 0 080 | 247 | >70 | 224 | 967 |
| WC-Co | Mettech | 0 080 | 780 | >70 | 162 | 659 |
| WC-Co | Metcon | 0.140 | 548 | 46 | 227 | 732 |

jig; that is, a "free" grit-blasted foil that was not attached to a substrate. The nonzero "peel strength" in this case (Fig. 1d) accounts for the work of plastic deformation of the peeled foil, the alignment dead weight, and the frictional losses in the loading system. The level of variation of ±10 N/m on this peel strength curve represents the expected level of experimental noise in the PAT. Any variation beyond this level originates in real variation in the peel strength and can be traced to interfacial faults. All data in Fig. 2 to 8 were obtained by subtracting the respective calibration curve from the raw data obtained from the tests.

The following section shows that typical short range (<1 mm of peel distance) variations of peel strength for TSC are within ±50 N/m. The long-range variations of peel strength for TSC (10 to 20 mm of peel distance) could reach ±400 N/m, reflecting the major effects of particle velocity and temperature, and residual thermal stresses in the coating on adhesion. The contribution of plastic deformation of the foil to the peel work was modeled and calibrated; these results are detailed in a separate work (Ref 10). From the load-displacement curve, the peel strength was calculated as a function of crack position.

## 4. Results of PAT for Various TSC

The peel curves for representative samples of the coatings studied in this work are compiled in Fig. 2 and 3 for WC-Co TSC, Fig. 4 and 5 for $Cr_2O_3$, Fig. 6 for Ti, and Fig. 7 and 8 for bond coats. Table 1 summarizes the representative results. For comparison, the peel strength of a uniform coating is averaged over 30 mm of peeling. This arbitrary distance was chosen because it is larger than the usual width of the spray pattern and, thus, is larger than the scale of the expected variability. For profile coatings, the entire curve must be reported because the variation is important. Many peel tests were performed on a variety of coatings on both Ni and stainless steel substrates. To elucidate the significance of each curve, two examples are discussed in terms of how they indicate coating quality and process features.

### 4.1 *PAT Results for WC-Co TSC*

Figures 2 and 3 show the peel curves for a WC-17wt%Co coating sprayed by the axial injection torch on Ni (Fig. 2a for uniform coating and Fig. 2b for profile sample) and stainless steel (Fig. 3a for uniform coating and Fig. 3b for profile sample). Figure 2(a) shows the peeling curve for the uniform coating sample on Ni. The initial position of the torch axis was at 40 mm, and the torch traversed toward decreasing position coordinate. Note that the adhesion drops in the direction of the torch traverse, from ~800 to ~600 N/m. This drop is accompanied by a visible color change on the fracture surface. The drop is likely due to longer exposure time of the low adhesion region to the spray environment. The surface would have been exposed to more of the fume in the spray booth than the regions covered earlier. It consists mainly of original powder fines, entrapped dust, and

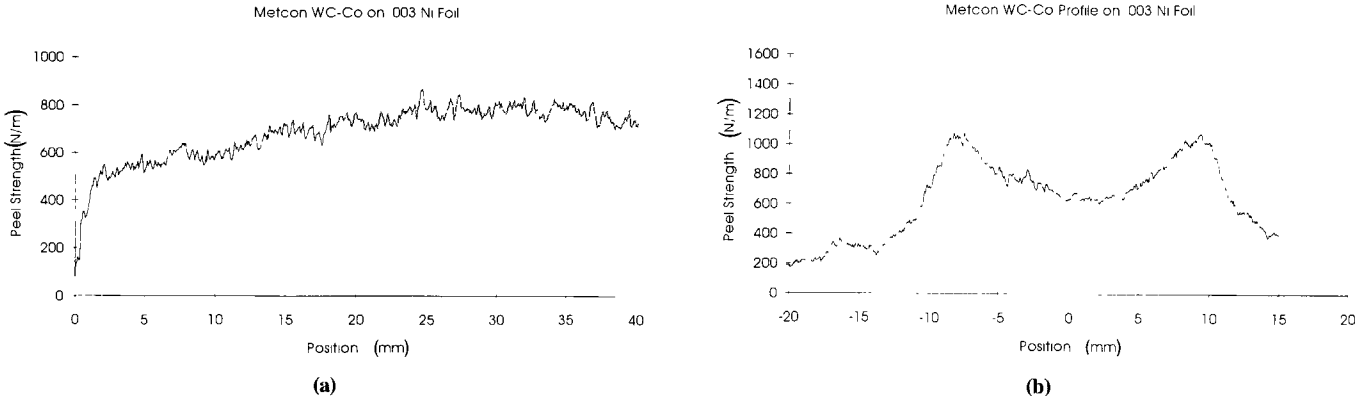


**Fig. 2** PAT results for plasma-sprayed WC-17wt%Co on Ni. (a) uniform coating and (b) spray profile

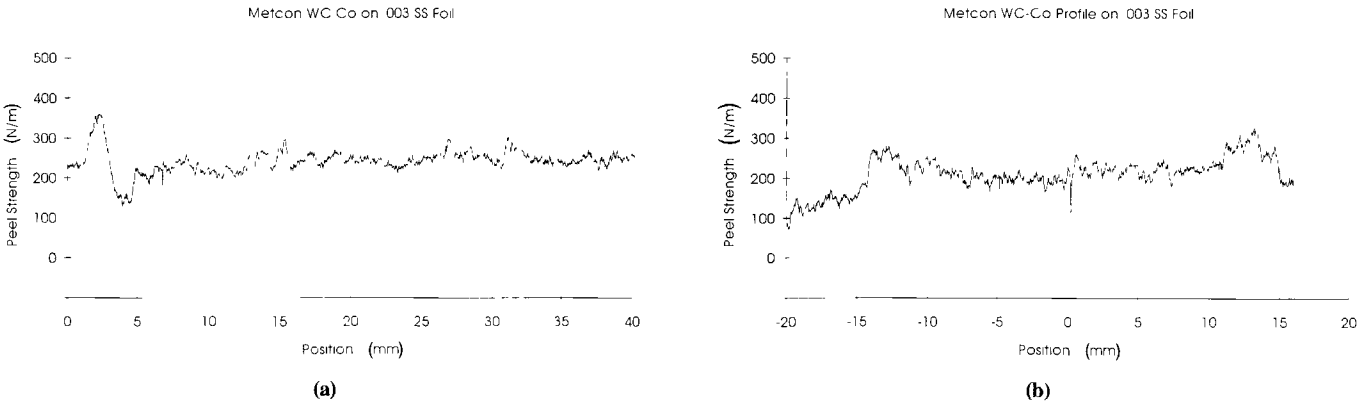


**Fig. 3** PAT results for plasma-sprayed WC-17wt%Co on stainless steel (a) uniform coating and (b) spray profile

condensed material from evaporated particles. Note that the effect of gradually decreasing peel strength in the direction of torch traverse is observed only for relatively high adhesion, for example, 600 to 700 N/m for WC-17wt%Co on Ni (Fig. 2a). The same coating on stainless steel (Fig. 3a) or ceramic coatings on various substrates (Fig. 4a and c, Fig. 5a) exhibit much lower adhesion across the peel distance, and no particular trend is observed.

The adhesion profile of the coating (Fig. 2b) shows a much larger variation than the uniform coating. The adhesion curve is symmetrical about the spray pattern center (position = 0 mm) where the deposit is thickest. In the peripheries, the adhesion slowly increases as one moves toward the center and reaches a maximum of 1000 N/m at 7 mm from the center. The adhesion then drops to 580 N/m in the center. This pattern may be due to the expected increase in residual stress with coating thickness. In the periphery, the coating is thin, and residual stresses are low. The peel strength increases toward the center due to the better processing of particles in more central parts of the pattern (Ref 14) but begins to decrease when residual stresses become large enough to assist in interfacial cracking. A second explanation is that the spray process has not been properly optimized for adhesion and that the majority of the particles traveling through the central portion of the pattern are too hot or fast to bond properly. These observations are not possible with any other test method. The uniform coating of WC-17wt%Co on stainless steel (Fig. 3a) exhibits a peel strength of ~200 N/m, which is at least a factor of 3 lower than the same coating on Ni. The profile sample in Fig. 3(b) shows a much smaller variation in the peel strength of the center and periphery as compared to the Ni substrate.

## 4.2 *PAT Results for Chromia TSC*

Figures 4(a) and (b) show the peel strength curve for a Rokide chromia coating sprayed onto a Ni foil. As expected for a brittle ceramic, it shows a much lower interfacial fracture energy than the metal and cermet coatings. The uniform coating curve (Fig. 4a) shows a constant bonding across the whole sample of ~220 N/m. Some small scale variations are present, which

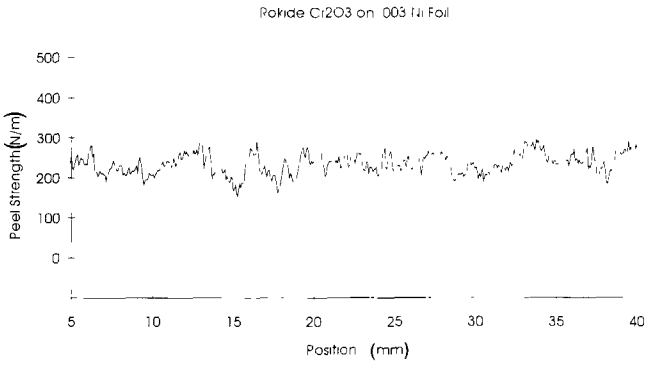


(a)

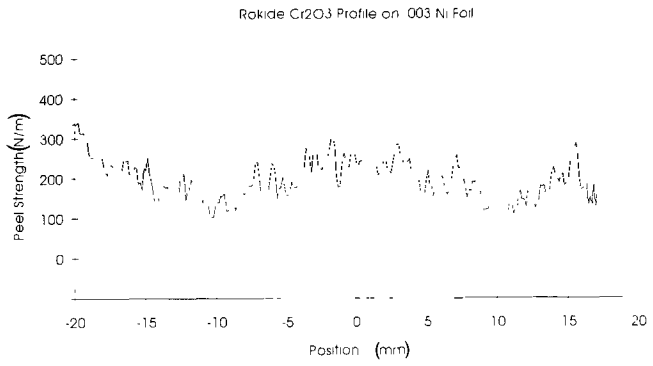


(b)

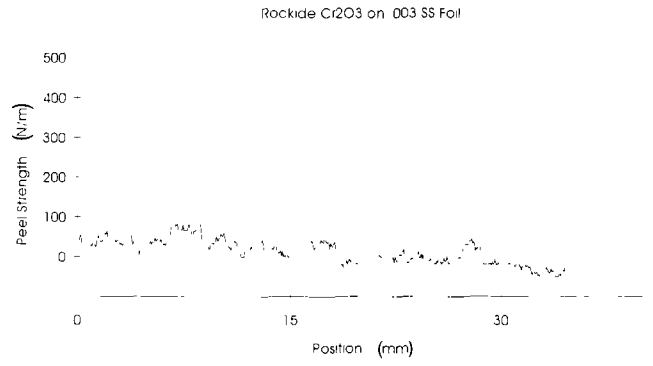


(c)

**Fig. 4** PAT results for chromium oxide sprayed by Rokide torch (a) uniform coating on Ni, (b) spray profile on Ni, and (c) uniform coating on stainless steel

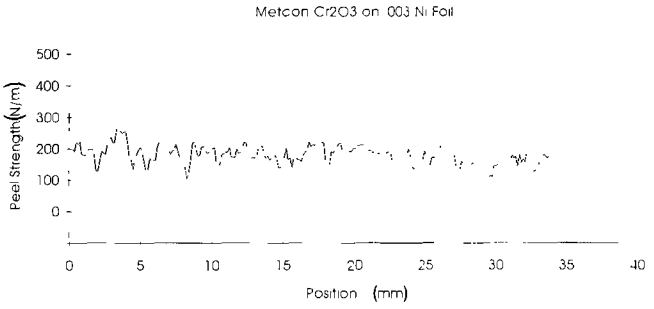


(a)

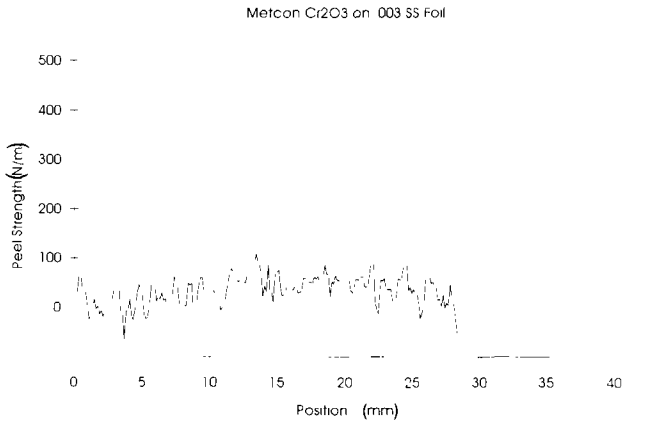


(b)

**Fig. 5** PAT results for plasma-sprayed chromium oxide: (a) uniform coating on Ni and (b) uniform coating on stainless steel

show no pattern. The profile shown in Fig. 4(b) shows that adhesion at the edges of the profile (±16 mm) is high and is very close to the level of adhesion of the epoxy used to bond the coatings to the Al plate. The coating is very thin in these regions, and the glue penetrates to the interface. As the coating becomes thicker, the adhesion drops as less glue is able to penetrate, and eventually penetration stops at coordinates ±10 mm. The minimum adhesion is ~140 N/m. The adhesion then begins to rise close to the center of the profile. The majority of the mass of the coating (~90%) is the region of rising adhesion. This is likely due to the optimized processing of the particles that travel through the central portion of the flame. The effects of residual stresses on peel adhesion are not noticeable for this coating. The peak level of adhesion occurs at the center of the profile and is ~260 N/m. The adhesion of the uniform coating (Fig. 4a) is much closer to the profile maximum than the profile minimum. This indicates that when producing uniform coatings, a small amount of "periphery particles" is mixed with a large amount of "center particles" to avoid influencing the adhesion strength of coatings. The same Rokide chromia coating uniformly deposited on stainless steel (Fig. 4c) exhibits significantly decreased adhesion, oscillating between 0 and 100 N/m. This is consistent with the above data for WC-17wt%Co. Figures 5(a) and (b) illustrate the peel adhesion of plasma sprayed chromia on Ni and stainless steel foils. The results are in a range similar to that of the Rokide system, especially regarding the low level of adhesion on stainless steel. Compare Fig. 5(b) and 4(c).

### 4.3 *PAT Results for Titanium TSC*

The PAT results for thermal sprayed Ti coatings are illustrated in Fig. 6(a) and (b) for Ni substrate and Fig. 6(c) and (d) for stainless steel substrate. The pattern of adhesion strength of the uniform Ti profile in Fig. 6(a) is similar to the one taken for WC-Co cermet in Fig. 2(a). Specifically, the strength of the coating deposited at the initial location of the torch (e.g., at position 25 to 30 mm) averages ~1100 N/m, to subsequently decrease to 800 to 900 N/m along the path of the torch. The respective strength of the profile Ti coating also is shaped similar to the cermet; the strength of the central region oscillates between 1000 and 1200 N/m and exhibits strong local variation in adhesion. Similar coatings deposited on 302 stainless steel foil produce significantly lower adhesion; that is, 150 to 300 N/m for the uniform coating (Fig. 6c) and 100 to 200 N/m for the central part of the profile (Fig. 6d).

### 4.4 *PAT Results for Bond Coats*

Figure 7 illustrates the peel strength of Ni-Fe-Al AMDRY 959 composite bond coat (Sulzer Plasma Technik, Inc., Troy, MI) sprayed on Ni (Fig. 7a and b) and on stainless steel (Fig. 7c and d) using an axial injection torch. Similarly, as for any other coating, the test foil was separated exactly along the interface between the bond coat and the substrate. The strength values oscillate within 600 to 800 N/m for the uniform coating on Ni (Fig.

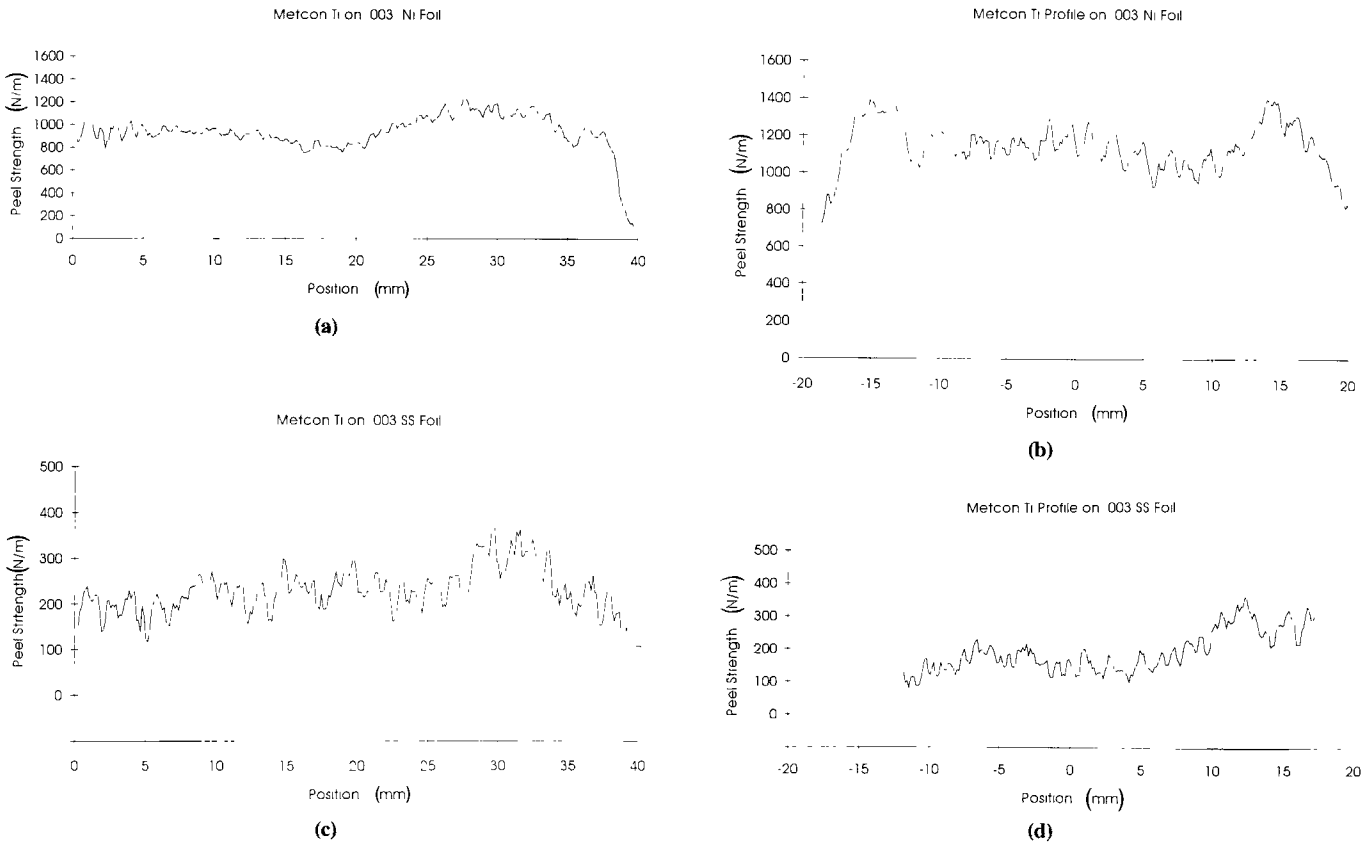


**Fig. 6** PAT results for plasma-sprayed titanium: (a) uniform coating on Ni, (b) profile coating on Ni, (c) uniform coating on stainless steel, and (d) profile coating on stainless steel

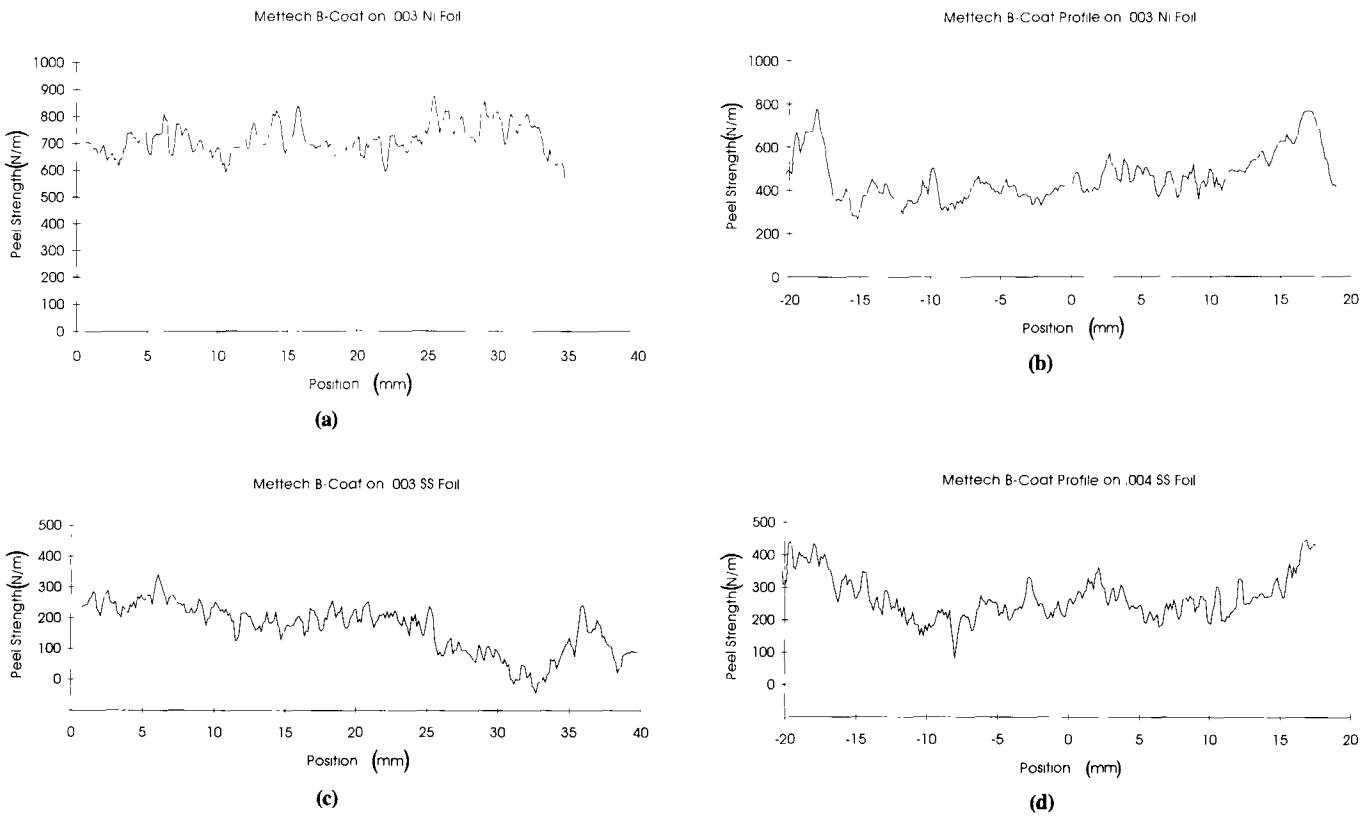


**Fig. 7** PAT results for plasma sprayed iron-base bond coat: (a) uniform coating on Ni, (b) profile coating on Ni, (c) uniform coating on stainless steel, (d) profile coating on stainless steel

7a) and 300 to 500 for the central part of the profile (Fig. 7b). The same uniform bond coat on stainless steel ranges in bond strength from ~250 to 0 N/m, along the torch traverse distance (Fig. 7c). The central part of the profile bond coat on stainless steel also had strength of 200 to 300 N/m (Fig. 7d).

Figures 8(a) and (b) represent the results of the PAT for alumina uniformly deposited on Rokide NiCr bond coat, using the Rokide torch and Ni and stainless steel foils. Because the foil was separated exactly along the interface between the bond coat and the substrate, these results are classified into testing the adhesion strength of bond coats. Consistent with all the previous results, the peel bond strength on Ni is higher by at least a factor of 2, as compared to the peel bond strength on stainless steel (i.e., 400 to 600 N/m versus 150 to 300 N/m, respectively).

## 5. Discussion

Several general observations about the peel test and the TSC are drawn from the results of this study. The peel test propagates a crack exactly along the coating substrate interface in a controlled, unique manner that can detect the location of bonding flaws, bonding changes with substrate material, and the required energy for failure. The detected parameter is self-consistent and can be correlated with other test results. The peel curves are not smooth, continuous curves and show significant variations. The test apparatus could be expected at worst to generate variations of 10% (Fig. 1d) . This would include measurement system noise, drift, and frictional variations. The variations larger than this must be considered significant, although there is no clear relationship between these variations and the crack propagation characteristics or microstructural features of the coating, substrate, or interface. Occasionally, large surface defects were visible, and these were correlated to the features of the peel curve. The noise is possibly indicative of a slip-stick type of crack propagation. The crack can only propagate a short distance before the stresses drop below the level required to continue cracking. Alternatively, the noise may reflect the variation in bond strength on a small scale.

At the outset of this study, it was expected that, due to the large differences in coating properties across the spray pattern, large differences in properties would exist in the adhesion of the coating. These variations should coincide with the torch path and thus be periodic in the torch traverse direction. A second possibility was that, on the first set of passes, the poorly processed periphery particles would land first and cause a lower adhesion than would be found in the center of the profile. The peel test did not indicate any long-range periodic changes in adhesion, and the adhesion of a uniform coating was not significantly lower than the maximum adhesion of the profile. Examination of the adhesion profiles indicates that the centers of the profiles generally have lower adhesion than the edges, especially for metallic and cermet coatings. This is likely due to the increased residual stress in the thicker, hotter portion of the profile. Thus, strategies for improving adhesion should be based on reducing residual stress rather than improving the processing of periphery particles.

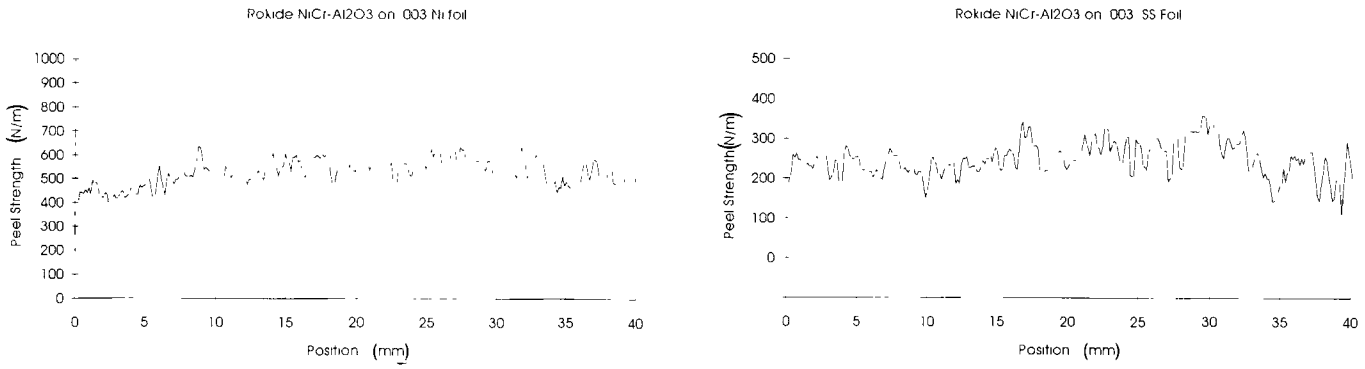


**Fig. 8** PAT results for Al oxide on NiCr bond coat sprayed by Rokide torch (a) uniform coating on Ni and (b) uniform coating on stainless steel

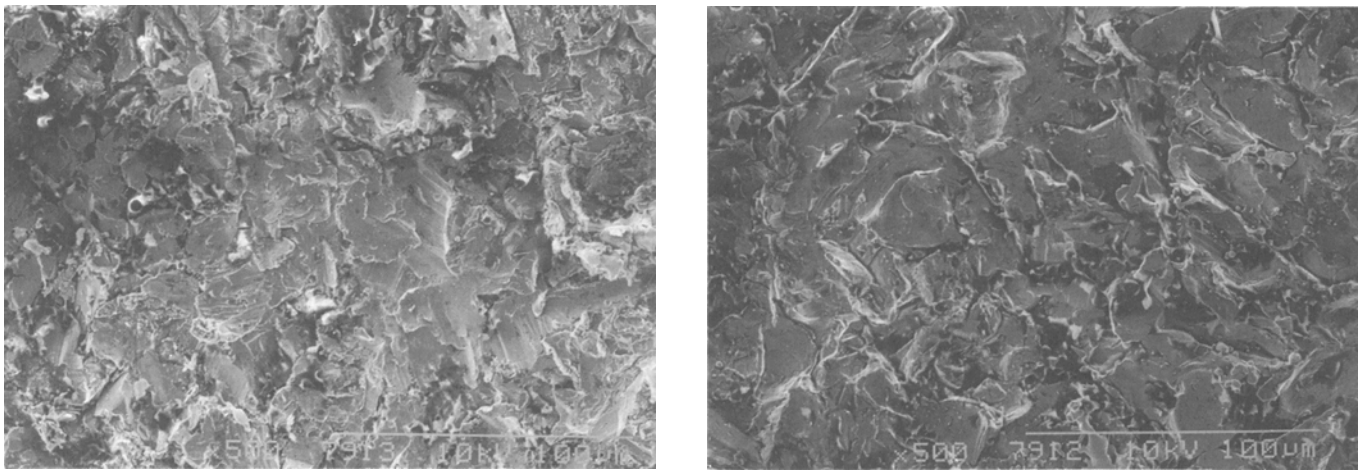


**Fig. 9** The substrate side of the interface fracture surface: (a) Ni substrate and (b) stainless steel substrate Both exhibited brittle fracture, but the Ni foil is qualitatively more ductile

The peel strength essentially represents the failure energy per unit area in terms of $J/m^2$, and it can be compared to the fracture toughness of coating interfaces. Several researchers (Ref 15-17) compiled a limited set of interfacial fracture toughness, $G_{IC}$, values for various coating systems from double cantilever beam (DCB) tests, which produce mode I (opening) stress at the crack tip in homogeneous materials. Because the peel test has a significant amount of mode II (sliding) stress at the crack tip, the results are not comparable as would be desired. Additionally, for the DCB fracture tests, the crack paths were usually through the coating or close to the interface, whereas PAT consistently causes failure on the interface. Caution should be employed in their interpretation. However, these differences should not significantly affect the range of possible values. Table 2 shows the typical range of values found for the DCB test and the peel test for both Ni and stainless steel foil. The peel strengths are generally of the same order of magnitude as the reported toughness for the steel substrate, but are at the higher end of the range. The toughness values for the Ni substrate are much higher than the other values by an approximate factor of 3.

In all cases, the peel strength for the Ni foil was much higher than for the stainless steel foil. The foils were prepared and sprayed in exactly the same manner; thus, some material difference must account for this difference. The increased peel strength may be due to the difference in the substrate chemistry. If this were the case, the difference would not likely occur with all of the different coating materials. The peel strength on Ni foil was always higher. During thermal spraying, molten splats cool in approximately $10^{-7}$ s (Ref 18). This is commonly used as an argument that no chemical reactions have time to occur, so the bonding of the TSC is independent of chemistry. A second possibility is that the lower yield strength and higher ductility of Ni allowed it to deform more easily upon particle impact, creating a better roughness during grit blasting and a better mechanical fit during spraying. This ductility also could reduce the residual stress level. During peeling, the extra energy required to deform the surface asperities would be reflected in a higher interface fracture energy and a more ductile fracture surface. SEM photo-

**Table 2 Comparison of fracture energies**

| Coating type | DCB test, $J/m^2$ | PAT on stainless steel, $J/m^2$ | PAT on Ni, $J/m^2$ |
|---|---|---|---|
| Ceramic | 10-100 | 10-60 | 175-275 |
| Cermet | 20-60 | 150-250 | 600-750 |
| Metal | 80-350 | 160-300 | 450-980 |

graphs of the fracture surfaces resulting from PAT (Fig. 9) show that both Ni and stainless steel substrates had a brittle fracture pattern, although the Ni substrate has more signs of ductile deformation on a local scale. If the ductility of the Ni substrate drastically improves the bond strength, as indicated by the peel test, then it offers a strategy for improving bond coat materials. This hypothesis, however, must be confirmed with other techniques. Currently, most thermal sprayed bond coats are complex alloys that are inherently less ductile than pure metals. A more ductile bond coat may improve bonding. Pure Al or other corrosion-resistant ductile metals thus may be useful bond coats in some applications.

The question of why the crack propagates along the interface and not some other lower energy path, such as through the coating, is difficult to answer. The special geometry of the test is likely the cause. Because of the small mandrel size, high foil strains are concentrated in a small region. The difference in the ability of the materials on each side of the interface to accommodate strain causes the stress field to be concentrated close to the interface. Models of the peel test (Ref 3, 4) indicate that the peel test geometry causes stress fields that force the crack to propagate along the interface. The crack follows the *local* lowest energy path, which is the interface. In this case, the "extra" toughness may come from the mechanisms that occur due to the rapidly increasing strains behind the crack tip. This explanation is overly simple, and a better understanding of crack propagation along highly strained rough interfaces is necessary. The experimental data, however, indicate that high energies are measured and that failure occurs exactly at the interface. This is a significant advantage of using the PAT for adhesion strength evaluation of the TSC.

Many coatings were tested, and it is possible to correlate the peel strength with both hardness and tensile bond strength. Table 1 summarizes the results of each test for several coatings. A general quantitative relationship between tensile bond strength determined through the tensile adhesion test (TAT) and peel strength determined through the PAT is not currently available, but as tensile bond strength increases, the peel strength should also increase. Because many of the TAT samples failed in the glue, indicating TAT strength >70 MPa, it is not possible to evaluate this relationship. The peel test is capable of testing coatings with much higher bond strengths than the TAT, such as those produced by the new generation of thermal spray processes. A second consistency check is that, in general, the peel strength on Ni should increase when the stainless steel peel strength increases; see Fig. 10(a). It is not possible to develop a relationship between the two peel strengths, but in most cases, they increase with each other.

A commonly used parameter for evaluating the general quality of a coating is Vickers hardness. This parameter reflects the properties of the coating material, the degree of porosity, the coherency, and the degree of microcracking. Because the effects of these are all combined in a complicated manner, it is not a very useful measurement for engineering predictions. The results of Vickers hardness testing (300 g load) are compiled in Table 1. Results indicate that harder coatings tend to adhere less well than softer coatings. This is consistent with the general wisdom about resistance to fracture of materials and, in particular, coatings. The lines in Fig. 10 indicate the trends although correlation is rather poor, especially for Ni substrates. For both the soft Ni substrate and the hard stainless steel substrate, adhesion decreases as the coating hardness increases (Fig. 10b). The same figure confirms clearly that the two different substrate materials have very different surface conditions, which strongly influence adhesion strength. These observations indicate that the peel test produces self-consistent results that fit with the current state of knowledge about coatings.

## 6. Conclusions

Several conclusions are drawn from the above development and the results of the PAT for TSC. The PAT data indicated several features of the TSC that are not possible to obtain by any other method. The peel test provides more information about how a coating can fail than most other destructive tests. It is thus a useful tool when doing developmental work on a coating. It allows the defects or regions of low adhesion to be precisely located and thus allows them to be studied for their cause. Repeatable measurements of the variations in adhesion within a coating were achieved that allow the test to be used for coating evaluation and comparison. The observed details of the variations may lead to a better understanding of the mechanism of failure along the coating/substrate interface. Failure occurs in the PAT exactly along the interface; thus, the test is a true reflection of adhesion and not the cohesion of the coating. Because the test is not limited by the strength of an organic bonding agent, it is capable of testing the adhesion of the high strength coatings, which previously were not testable.

The peel test results must be consistent with what is known about adhesion for the peel test to be accepted. The peel strengths measured here agree with other measurements of interfacial fracture toughness, $G_{IC}$, and are considered reasonable. It is believed that the peel test produces stress intensities similar to those encountered in coating service. The peel strength decreases with an increase in hardness. This is consistent with the fact that hard materials tend to fail in a low-energy brittle manner. The peel strength is consistent with itself in that the peel strength on one substrate increases with the peel strength on another. This is despite the fact that adhesion to the ductile Ni foil was much higher than adhesion to the hard stainless steel foil by about a factor of 3. As this is not likely due to chemistry, the ductility of the Ni substrate is likely the cause of the enhanced adhesion. This indicates that ductile bond coats may be advantageous over some of the harder alloys.

The peel test can also be useful as a quality assurance tool. It is less sensitive to sample size and alignment than the TAT (according to ASTM C 633), and it provides a more reliable evaluation of the coating quality. PAT is relatively easy to perform when compared to sophisticated fracture mechanics tests; thus, spray shops can do their own testing. The conditions of the test produce a stress intensity at the crack tip that is very similar to the type of stresses expected at an interface under bending loads or in-plane residual stresses. Therefore, the test causes failure in a manner similar to the typical causes of failure in coating applications. The peel strength measured in the PAT is thus more useful in predicting service constraints than the TAT, most fracture mechanics tests, or ultrasonic adhesion measurements.

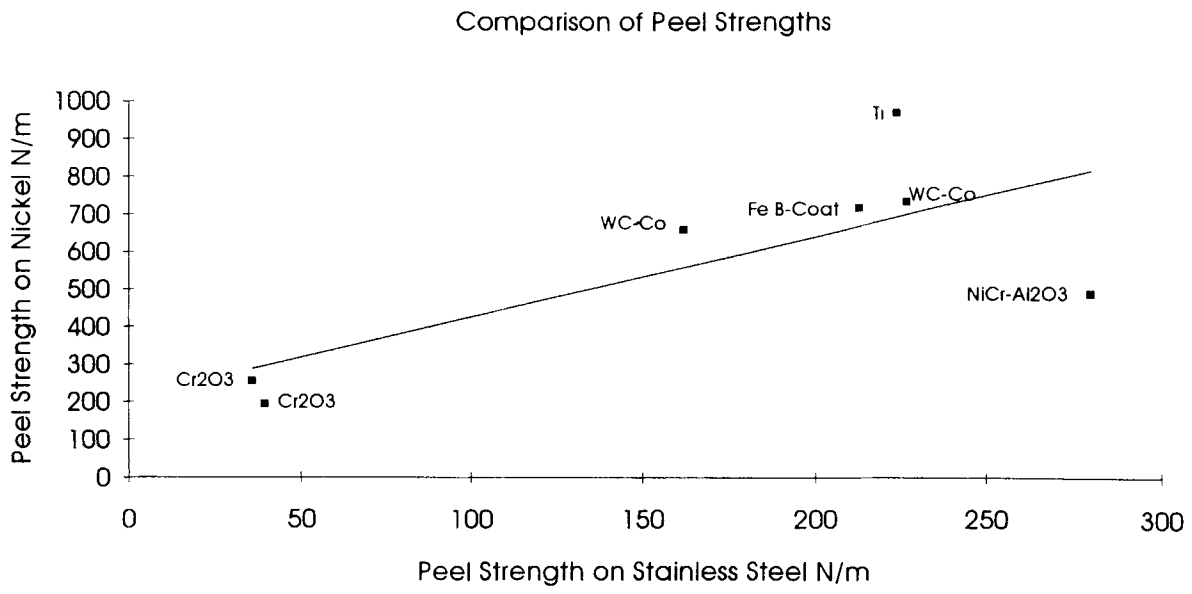


(a)

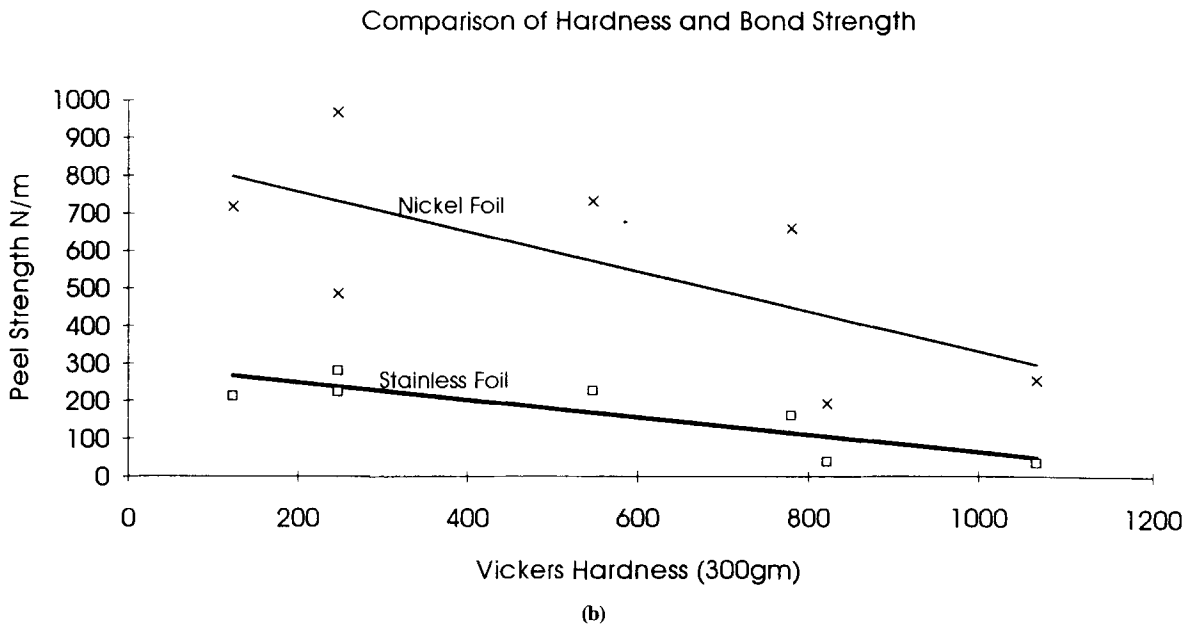


(b)

**Fig. 10** (a) A plot of peel adhesion on stainless steel versus the peel adhesion on Ni foil showing that an increase in adhesion to one substrate corresponds to an increase in adhesion to the other. Each point is labeled with the coating type (b) A plot of Vickers hardness (300 g load) versus adhesion showing that an increase in hardness corresponds to a decrease in interfacial energy. Each point represents a different coating type

The peel test can be improved. A major criticism is the need to solder the foil substrate to a back plate. A scheme is being developed to allow the foil to be held and cooled during spraying without solder. This would allow the testing of substrates that are difficult or impossible to solder, such as titanium. It would also reduce the preparation time associated with the test. To accomplish this, thicker foils and larger bending mandrels would be needed. A second improvement would be the development of a simple bench top testing jig, which does not require the expensive tensile machine and data acquisition system. A scaled-down version of the existing system would be adequate. This is currently the subject of continued development of the PAT.

The peel test has proven to be a useful adhesion measurement technique for the TSC. It has several advantages over conventional testing techniques that make it useful for both quality assurance and developmental testing. The results can be related to the parameters of fracture mechanics and are thus useful in predictive work. Further work is needed to develop a complete mechanical description of the system, to use the test result to improve the spraying process, and to determine the relationship between the test results and the performance of the coatings.

## Acknowledgments

The authors would like to thank the following industries for providing access to the processing equipment and spray powders: Northwest Mettech, Richmond, B.C. V6V 1M3; Metcon Services, Abbotsford, B.C. V2S 1M3; Norton, Worcester, MA

01615-0008. Financial support of the Science Council of British Columbia to this program is gratefully acknowledged.

## References


1. H S Ingham, Jr., Adhesion of Flame Sprayed Coatings, *Adhesion Measurement of Thin Films, Thick Films and Bulk Coatings,* K.L. Mittal, Ed , ASTM, 1976, p 285-291
2. "Standard Test Method for Peel or Stripping Strength of Adhesive Bonds," D 903-49, *Annual Book of ASTM Standards,* ASTM, 1983
3. "Standard Test Method for Floating Roller Peel Resistance of Adhesives," D 3167-76, *Annual Book of ASTM Standards,* ASTM, 1986
4. A.D. Crocombe and R D Adams, An Elasto-Plastic Investigation of the Peel Test, *J. Adhes.,* Vol 13, 1982, p 241-267
5. A.D. Crocombe and R D. Adams, Peel Analysis Using the Finite Element Method, *J. Adhes.,* Vol 12, 1981, p 127-139
6. M D. Thoules and H.M. Jensen, Elastic Fracture Mechanics of the Peel Test Geometry, *J. Adhes.,* Vol 38, 1992, p 185-197
7. K. Kim and J. Kim, Elasto-Plastic Analysis of the Peel Test for Thin Film Adhesion, *J. Eng. Mater. Technol.,* Vol 110, 1988 , p 266-273
8. J. Holowczak, V. Greenhut, and D Shanefield, Peel Adhesion Bond Strength of Direct Bonded Copper Alumina as Affected by Alumina Sintering Aids, *Met. Ceramic Joining,* P. Kumar and V. Greenhut, Ed., TMS/AIME, 1991, p 153-166
9. M. Sexsmith and T Troczynski, Peel Adhesion Test for Thermal Sprayed Coatings, *J. Therm. Spray Technol.,* Vol 3, 1994, p 404-411
10. M Sexsmith and T. Troczynski, Model for Plastic Deformation Work of Peeled Metallic Foils, *J. Adhes. Sci. Technol.,* to be published April 1996
11. M. Sexsmith and T Troczynski, Development of Peel Adhesion Test for Thermal Sprayed Coatings, *Proceedings of the 14th International Thermal Spray Conference* (Kobe), 1995, p 897-902
12. M. Sexsmith and T. Troczynski, Variations in Coating Properties across a Spray Pattern, *Proceedings of the 7th National Thermal Spray Conference* (Boston), 1994, p 751-757
13. "Standard Test Method for The Adhesion of Flame Sprayed Coatings," C 633-79, *Annual Book of ASTM Standards,* ASTM, 1979
14. J.R Finke and W.D. Swank, Simultaneous Measurement of Ni-Al Particle Size, Velocity, and Temperature in Atmospheric Thermal Plasmas, *Thermal Spray: International Advances in Coating Technology,* C.C. Berndt, Ed., ASM International, 1992, p 39-43
15. T. Troczynski and J. Camire, Resistance to Fracture of Thermal Sprayed Ceramic Coatings, *Thermal Spray Industrial Applications,* C Berndt and S. Sampath, Ed., ASM International, 1994, p 663-668
16. C.K. Lin and C.C. Berndt, Measurement and Analysis of Adhesion Strength for Thermally Sprayed Coatings, *J. Therm. Spray Technol.,* Vol 3 (No. 1), 1994, p 75-104
17. C. Berndt and R. McPherson, The Adhesion of Plasma Sprayed Ceramic Coatings to Metals, *Mater. Sci. Res.,* Vol 14, 1981, p 618-628
18. V.E Belaschenko, Thermal Conditions of Formation of Hot Sprayed Coatings on Flat Surfaces, *Fiz. Khim. Obrab. Mater.,* Vol 20 (No. 3), 1986, p 82-87